

Supplementary Information: Granular Metals with SiN_x Dielectrics

Simeon J. Gilbert,^{1*} Melissa L. Meyerson,¹ Paul G. Kotula,¹ Samantha G. Rosenberg,¹ Thomas G. Kmiecik,¹ Michael P. McGarry,¹ Michael P. Siegal,¹ and Laura B. Biedermann^{1*}

¹Sandia National Laboratories, Albuquerque, NM 87185, USA

*Corresponding Authors: sjgilbe@sandia.gov, lbieder@sandia.gov

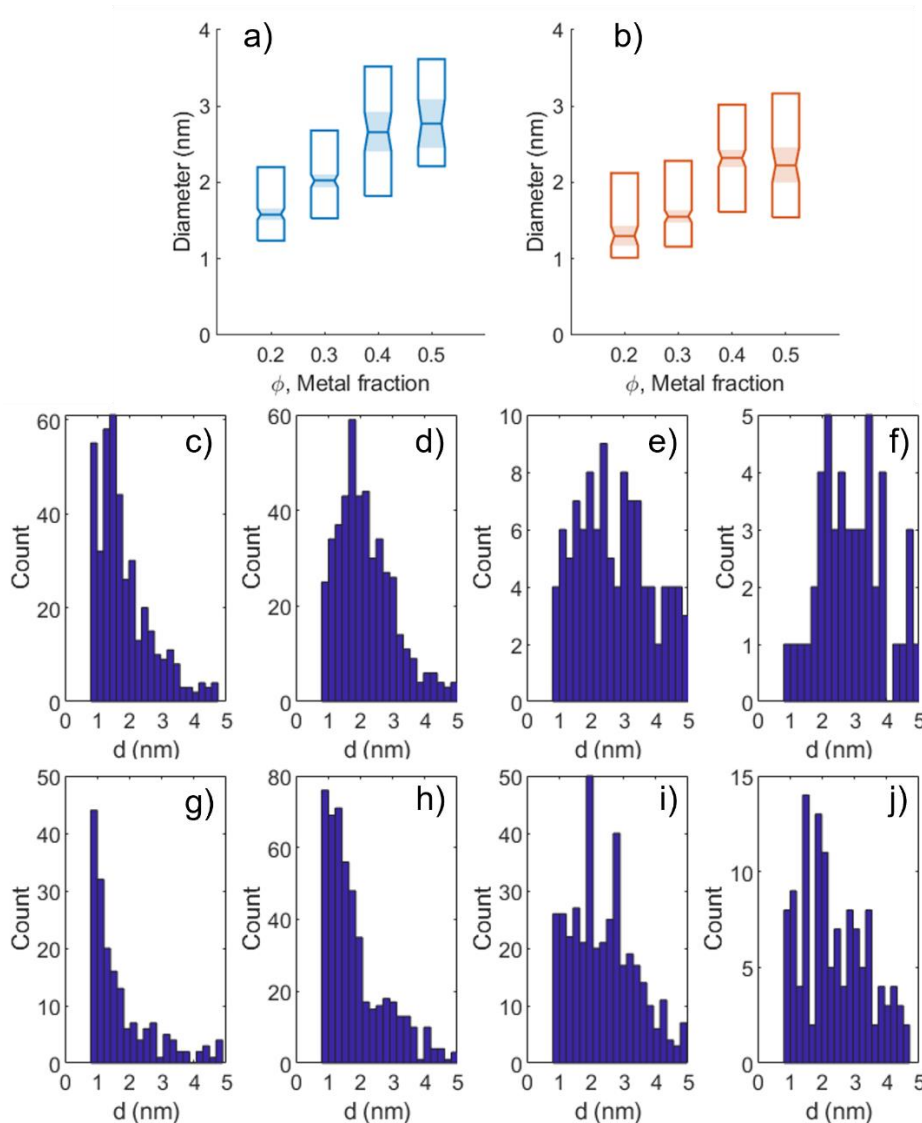


Figure S1. The distributions of the metal nanoparticle diameters in Co-SiN_x (a) and Mo-SiN_x (b) determined from analysis of the STEM images in Figure 1. The bottom, middle, and top horizontal lines show the 25th percentile, median, and 75th percentile measurements, respectively. The notched, shaded regions represent variability in the median. The medians are statistically different at the 5% significance level when these shaded regions do not visually overlap. Histograms of the nanoparticle diameters in Co-SiN_x (c-f) and Mo-SiN_x (g-j) for $\phi = 0.2$ (c,g), $\phi = 0.3$ (d,h), $\phi = 0.4$ (e,i), and $\phi = 0.5$ (f,j). The 1 and 5 nm limits are boundaries set by the image processing.

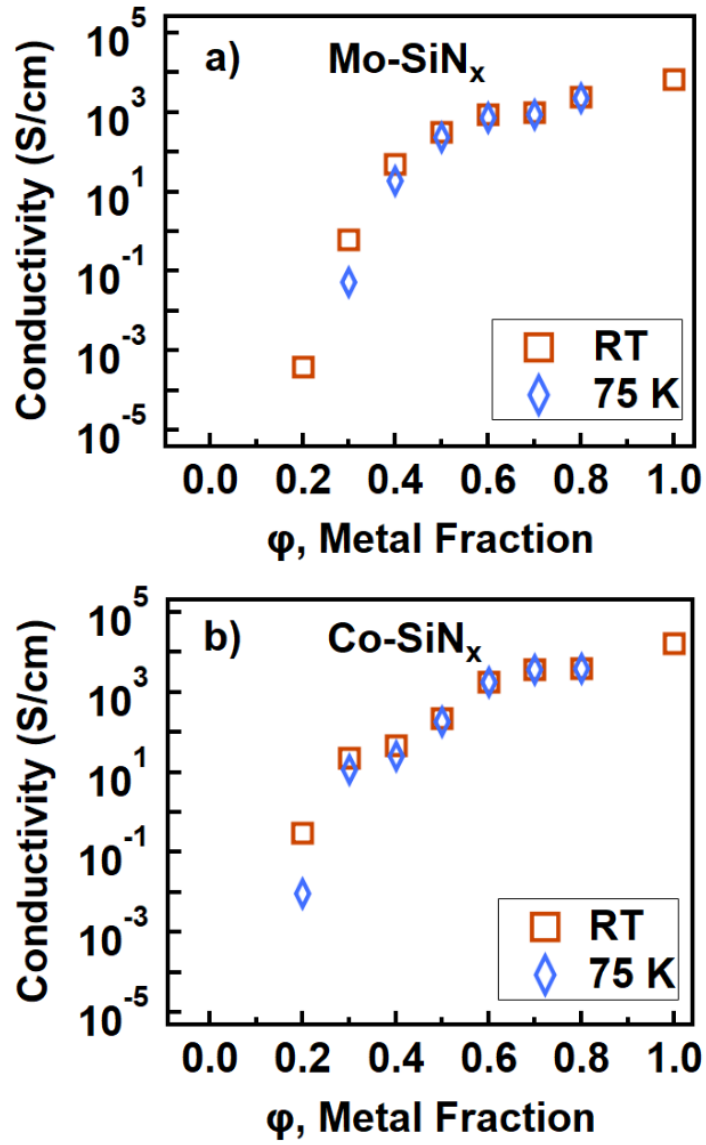


Figure S2. The conductivity of a) Mo-SiN_x and b) Co-SiN_x GMs with varying volumetric metal fractions (ϕ) at room temperature and 75 K. Below the percolation threshold (ϕ_c), conduction occurs through thermally assisted tunneling and should decrease at lower temperatures. For $\phi \geq 0.5$, there is minimal difference in conductivity between room temperature and 75 K, which suggests ϕ_c is near 0.4.

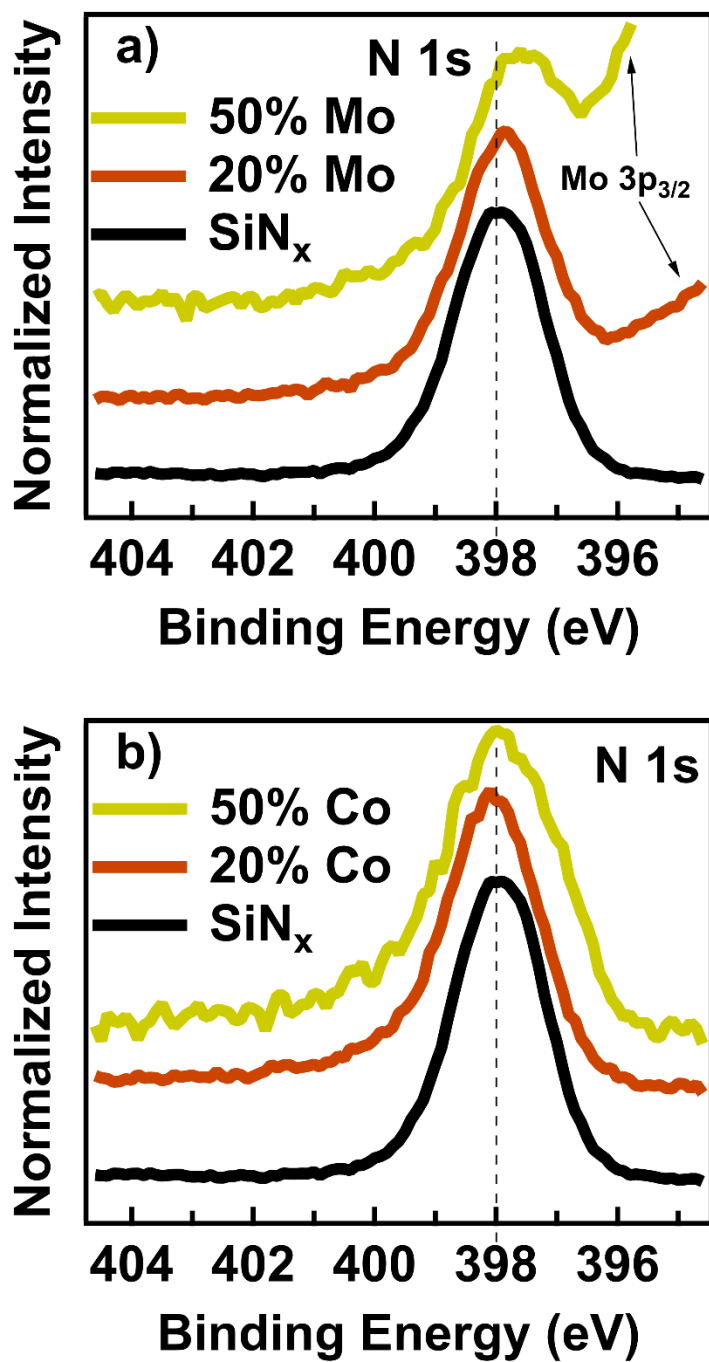


Figure S3. The N 1s XPS peaks in a) Mo-SiN_x and b) Co-SiN_x with varying volumetric metal fractions. The dotted line denotes the binding energy of the pure SiN_x films.

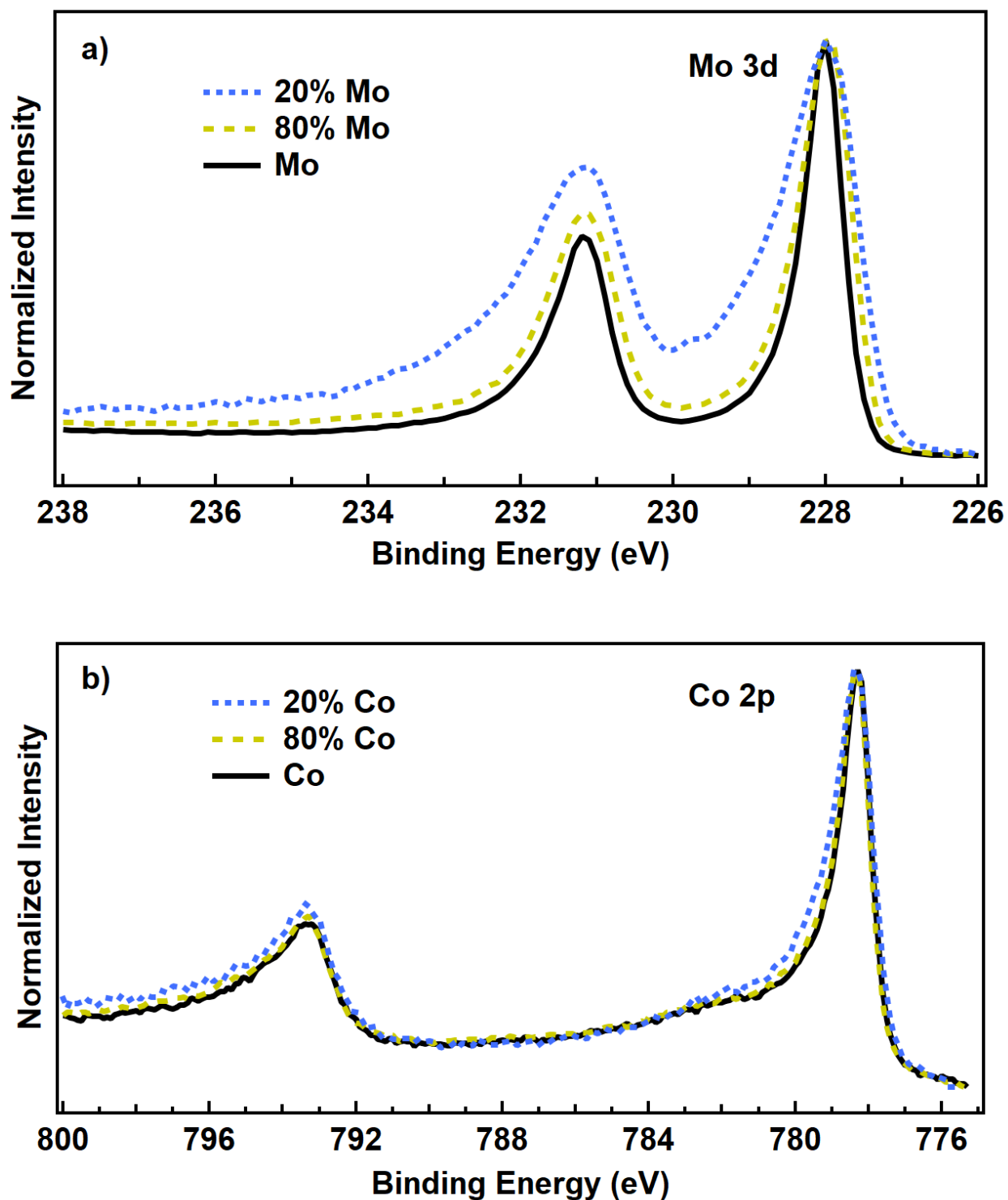


Figure S4. a) the Mo 3d XPS peaks for Mo-SiN_x with varying ϕ . b) The Co 2p XPS peaks for Co-SiN_x with varying ϕ . The FWHM of the Mo 3d and Co 2p XPS peaks increases as ϕ decreases. This broadening is likely the result of metal-silicide and metal-nitride formation and is more exaggerated in the Mo-SiN_x GMs than in Co-SiN_x.

ACKNOWLEDGEMENTS

This work was supported by the Laboratory Directed Research and Development (LDRD) program at Sandia National Laboratories. Sandia National Laboratories is a multimission laboratory managed and operated by National Technology and Engineering Solutions of Sandia, LLC (NTESS), a wholly owned subsidiary of Honeywell International Inc., for the U.S. Department of Energy's National Nuclear Security Administration under contract DE-NA0003525. This written work is authored by an employee of NTESS. The employee, not NTESS, owns the right, title and interest in and to the written work and is responsible for its contents. Any subjective views or opinions that might be expressed in the written work do not necessarily represent the views of the U.S. Government. The publisher acknowledges that the U.S. Government retains a non-exclusive, paid-up, irrevocable, world-wide license to publish or reproduce the published form of this written work or allow others to do so, for U.S. Government purposes. The DOE will provide public access to results of federally sponsored research in accordance with the DOE Public Access Plan.